

Sustainable Development of Civil, Urban and Transportation Engineering Conference

## Effect of Different FRP Wrapping Arrangements on the Confinement Mechanism

Thong M. Pham<sup>a</sup>, Jim Youssed<sup>b</sup>, Muhammad NS Hadi<sup>b</sup> and Tung M. Tran<sup>c,\*</sup>

<sup>a</sup>*School of Civil and Mechanical Engineering, Curtin University, Kent Street, Bentley, WA 6102, Australia*

<sup>b</sup>*School of Civil, Mining, and Environmental Engineering, University of Wollongong, Wollongong, NSW 2522, Australia*

<sup>c</sup>*Faculty of Civil Engineering, Ton Duc Thang University, 19 Nguyen Huu Tho St., Dist. 7, HCMC 700000, Viet Nam.*

### Abstract

This study aims to investigate the structural behavior and failure modes of fiber-reinforced-polymer (FRP) confined concrete wrapped with different FRP arrangements. A total of twenty four specimens were cast and tested, with three of these specimens acting as reference specimens and the remaining specimens wrapped with different types of FRP (CFRP and GFRP) by different wrapping arrangements. They include fully wrapped, partially wrapped and non-uniformly wrapped concrete cylinders. The non-uniformly wrapped concrete cylinders provided higher compressive strengths and strain for FRP-confined concrete, in comparison with conventional fully wrapping arrangements. The effect of confinement level on the effectiveness of FRP confinement is also investigated. In addition, the partially wrapping arrangements changes the failure modes of the specimens and the angle of the failure surface.

© 2016 The Authors. Published by Elsevier Ltd. This is an open access article under the CC BY-NC-ND license (<http://creativecommons.org/licenses/by-nc-nd/4.0/>).

Peer-review under responsibility of the organizing committee of CUTE 2016

*Keywords:* Fiber Reinforced Polymer; Confinement; Concrete columns; Strain; Stress-strain relation; Concrete; Cylinders.

### 1. Introduction

Fiber Reinforced Polymer (FRP) has been commonly used to strengthen existing reinforced concrete (RC) columns in a few decades. Most of the studies in the literature focus only on columns fully wrapped with FRP. Accordingly, the available design guidelines for columns wrapped with FRP, for example ACI 440.2R-08 [1]; Fib [2] and TR 55 [3], are utilized to estimate the capacities of partially FRP-wrapped specimens. Among these studies,

\* Corresponding author. Tel.: +84 915791597.

E-mail address: [tranminhtung@tdt.edu.vn](mailto:tranminhtung@tdt.edu.vn)

ACI 440.2R-08 [1] and TR 55 [3] do not provide information about the confinement effect of concrete columns partially wrapped with FRP. Meanwhile, Fib [2] suggests a reduction factor to take into account the effect of partial wrapping columns. The study by Fib [2] adopts an assumption proposed by Mander et al.[4] for the confinement effect of steel ties in RC columns to analyze the efficacy of FRP partially wrapped columns. Therefore, there has been a lack of theoretical and experimental works about partial FRP-confined concrete. For this reason, an experimental program was developed in this study to compare the confinement efficacy of FRP partially wrapped columns and FRP fully wrapped columns. The same amount of FRP was wrapped onto identical concrete columns by different wrapping arrangements to achieve an optimized wrapping design.

## 2. Confinement mechanism

The confinement mechanism of FRP confined concrete was presented for both cases including full and partial confinement in the study by Pham et al. [5]. When a circular concrete column is horizontally wrapped with FRP around its perimeter, the whole column is confined by the lateral pressure from the FRP jackets as shown in Fig. 1a. Many studies have been carried out to investigate the behaviors and estimate the capacities of columns wrapped fully with FRP [6-10]. The distribution of the confining pressure is assumed to be uniform in the cross section and along the axial axis of the circular columns. Among the existing studies, the model proposed by Lam and Teng [11] is adopted in this study to calculate the compressive strength for columns fully wrapped with FRP as follows:

$$\frac{f'_{cc}}{f'_{co}} = 1 + 3.3 \frac{f_l}{f'_{co}} \quad (1)$$

where  $f'_{cc}$  and  $f'_{co}$  are respectively the compressive strength of confined concrete and unconfined concrete, and  $f_l$  is the effective confining pressure as follows:

$$f_l = \frac{2E_f \varepsilon_{fe} t}{d} \quad (2)$$

where  $E_f$  is the elastic modulus of FRP,  $t$  is the nominal thickness of FRP jacket,  $d$  is the diameter of the column section, and  $\varepsilon_{fe}$  is the actual rupture strain of FRP in the hoop direction. The model by Lam and Teng [11] is chosen because it provides a reasonable accuracy with a very simple form. The simplicity of the model by Lam and Teng [11] is utilized to establish a new and simple strain model, which is presented in the sections below. The strain model proposed by Pham and Hadi [12] is adopted to calculate the compressive axial strain of confined concrete as follows:

$$\varepsilon_{cc} = \varepsilon_{co} + \frac{2ktf_{fe}\varepsilon_{fe}}{df'_{co} + 3.3tf_{fe}} \quad (3)$$

where  $\varepsilon_{cc}$  is the ultimate axial strain of confined concrete,  $\varepsilon_{co}$  is the axial strain at the peak stress of unconfined concrete,  $k = 7.6$  is the proportion factor, and  $f_{fe}$  is the actual rupture strength of FRP.

As mentioned above, the concrete columns wrapped partially with FRP have been experimentally verified to increase their strength and ductility. Concrete columns partially wrapped with FRP are less efficient in nature than fully wrapped columns as both confined and unconfined zones exist (Fig. 1b). An approach similar to the one proposed by Sheikh and Uzumeri [13] was adopted to determine the effective confining pressure on the concrete core. The effective confining pressure was assumed to be exerted effectively on the part of the concrete core where the confining pressure has fully developed due to the arching action as shown in Fig. 1b. In such a case, a confinement effective coefficient ( $k_e$ ) was introduced to take the partial wrapping into account as follows:

$$k_e = \frac{A_e}{A_c} = \left(1 - \frac{s}{2d}\right)^2 \quad (4)$$

where  $A_e$  and  $A_c$  are respectively the area of effectively confined concrete core and the cross-sectional area, and  $s$  is the clear spacing between two FRP bands. Consequently, the compressive strength of concrete columns wrapped partially with FRP could be calculated as:

$$\frac{f'_{cc}}{f'_{co}} = 1 + 3.3k_e \frac{f'_l}{f'_{co}} \quad (5)$$

where  $k_e$  is estimated based on Eq. 4 and  $f'_l$  shown in the following equation is the equivalent confining pressure from the FRP, assumed to be uniformly distributed along the longitudinal axis of the column.

$$f'_l = \frac{2E_f \varepsilon_{fe} t}{D} \frac{w}{w + s} \quad (6)$$

where  $w$  is the width of FRP bands.

### 3. Experimental program

#### 3.1. Test matrix

A total of twenty one FRP confined concrete cylinders and three reference unconfined specimens were made and tested under monotonic loading. The dimensions of the concrete cylinder specimens were 150 mm in diameter and 300 mm in height. All the specimens were cast from the same batch of concrete which had a compressive strength of 54 MPa at 28 days.

The experimental program consists of three groups of cylinders in order to evaluate the confinement efficacy between partially and fully wrapping arrangements in terms of optimization of the wrapping arrangement. The notation of the specimens includes three parts: the first part indicates the type of confining FRP material, with “G” and “C” representing GFRP and CFRP respectively. The second part is either a letter “R”, “F”, or “P” stating the name of the sub-group, namely, reference group (R), fully wrapped group (F) and partially wrapped group (P). The last part of the specimen notation is a number which specifies the number of FRP layers. Details of the specimens and wrapping arrangements are presented in Table 1.

Table 1. Test matrix

Group	No. of specimens	Type of FRP	Equivalent FRP layers with full wrapping	Width of each FRP band (w, mm)	Clear spacing (s, mm)
R	3	-	-	-	-
GF2	3			50	0
GP40	3	GFRP	2	25	25
GP31	3			25	0
CF3	3			75	0
CP60	3	CFRP	3	25	25
CP51	3			25	0
CP42	3			25	0

#### 3.2. Test setup

The hoop strains of the FRP bands were measured by three strain gages with a gage length of 5 mm. They were fixed at the mid height of the specimens and evenly distributed away from the overlap for the fully wrapped specimens. In the partially wrapped specimens, three strain gages were bonded symmetrically on a tie band and other three were bonded on a cover band at mid-height of the specimen. A longitudinal compressometer was used to measure the axial strain of the specimens. A Linear variable differential transformer (LVDT) mounted on the upper ring of the compressometer to measure the axial strain. The apparatus is presented in Fig. 2.

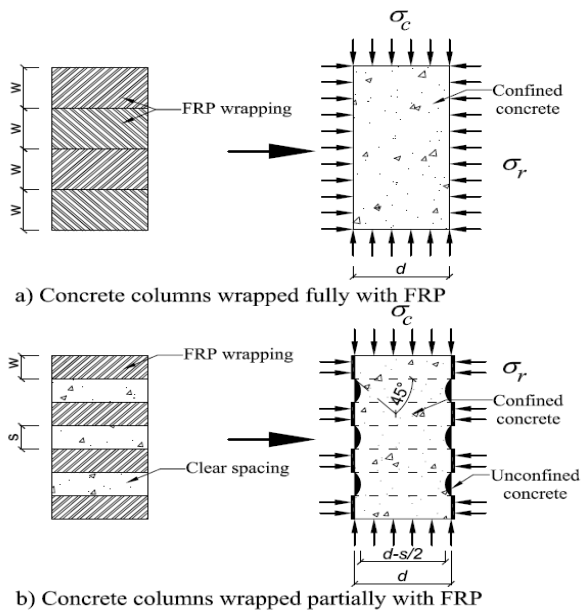


Fig. 1: Confinement mechanism



Fig. 2: Testing apparatus

The compression tests for all the specimens were conducted by using the Denison 500 tons capacity testing machine. High strength plaster was used to cap the specimen to ensure full contact between the loading plate and the specimen. Calibration was carefully carried out to ensure that the specimens were positioned at the center of the testing machine. Each specimen was first loaded to around 30% of its unconfined capacity to check the alignment. If required, the specimen was unloaded, realigned, and loaded again. The deflection controlled with a rate of 0.5 mm/min was used when conducting these tests. The readings of the load, LVDT and strain gages were recorded using a data logging system.

## 4. Experimental results and discussion

### 4.1. Failure modes of the tested specimens

As expected, the specimens fully wrapped with FRP (CF3 and GF2) failed by rupture of FRP at the mid-height. The failure surface of the fully wrapped specimens was observed at approximately 45 degree inclined, as shown in Fig. 3a. In the meantime, the partially wrapped specimens (CP60 and GP40) showed many small cracks on the concrete surface at a stress level that is equal to the unconfined concrete strength, as shown in Fig. 3b. The concrete between the FRP bands, which was close to the outer surface of the specimen, started crushing while the concrete core was still confined by the FRP bands. Accordingly, cracks on the concrete surface developed as the applied load increased (Fig. 3c). When the stress reached a certain high level, the concrete between the FRP bands spalled off while the concrete under the FRP bands and the core were still confined. These specimens then failed explosively by FRP rupture at the mid-height as shown in Fig. 3d.

The angle of the failure surface with respect to the horizon for the partially and fully wrapped specimens was significantly changed. As can be seen from Fig. 3d, the failure surface was observed at the spacing between FRP bands. This change of the failure surface depends on the wrapping arrangements and the stiffness of the FRP bands. When the axial stress of the confined concrete was higher than the unconfined concrete strength, the 45 degree failure surface may have originally transpired in the concrete cores, but cracks were arrested by FRP bands under the high stress stage. If the FRP bands is not stiff enough (Specimen GP40) to prevent the development of the cracks, the failure surface takes place at approximately 45 degrees as shown in Fig. 3e. On the contrary, the stiffness of the FRP bands in Specimen CP60 was strong enough so that it transformed the failure surface as depicted in Fig.

3d. It is worth mentioning that the stiffness of the FRP bands affects the tangent modulus of FRP-confined concrete. The low value of the tangent modulus causes column stability collapse directly as the unconfined concrete strength level is exceeded.

In addition, specimens with optimized non-uniform wrapping arrangements exhibited a different failure mode from the others. When the stress level is equal to the unconfined concrete strength, the concrete was still confined by the FRP tie bands and cover bands. During the loading process, the lateral strains of the tie bands and the cover bands were almost identical. The failure modes of these specimens are thus similar to those of the fully wrapped specimens. The non-uniformly wrapped specimens failed by FRP rupture simultaneously at the two bands (tie band and cover band) at the mid-height, as shown in Fig. 3f.

4.2. Stress-strain relationship

Stress-strain relationship of the tested specimens are divided into two main types based on the shape of the stress-strain curves, which are the ascending branch type and descending branch type. When a FRP confined concrete column is heavily confined, its compressive strength and strain are significantly higher than those of the unconfined concrete. Otherwise, FRP confined concrete with a stress-strain curve of the descending type illustrates a concrete stress at the ultimate strain below the compressive strength of unconfined concrete. Specimens wrapped with GFRP are designed to behave as the descending branch type while specimens wrapped with CFRP belong to the ascending branch type.

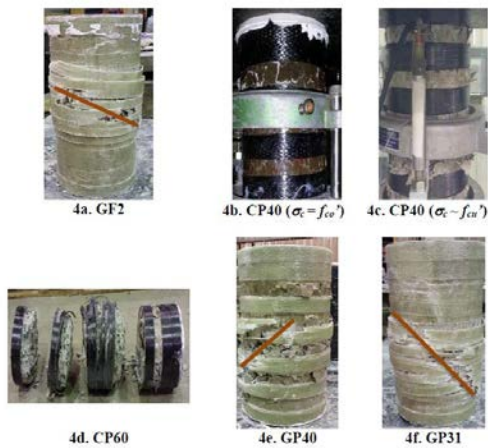


Fig. 3: Failure modes

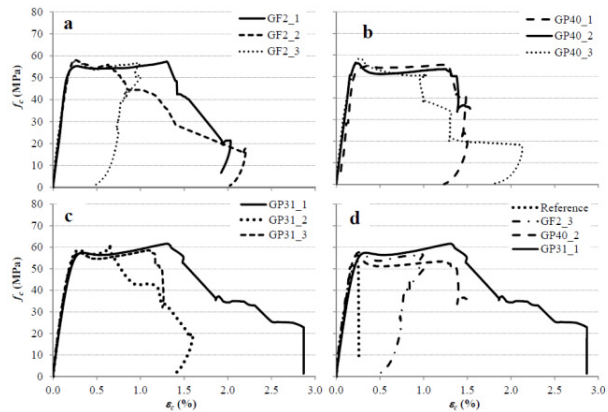


Fig. 4: Stress-strain curves of the specimens wrapped by equivalent two GFRP layers

Stress-strain curves of the specimens wrapped by equivalent two GFRP layers are presented in Fig. 4. The specimens which were wrapped with an equivalent of two layers of FRP had identical stress-strain curves at the early stages of loading and experienced slight differences at the latter stage of testing. For specimens wrapped by the same amount of FRP, Specimens GF2 and GP40 had the descending branch type stress-strain curve while the stress-strain curves of Specimens GP31 kept constant after reaching the unconfined concrete strength and then increased again to failure. The axial stress of Specimens GF2 reached the unconfined concrete strength of 54 MPa and then kept constant until the FRP failed by rupture as shown in Fig. 4a. The average compressive concrete strength and strain of Specimens GF2 were 57 MPa and 0.97 %, respectively. Although Specimens GP40 reached a lower maximum stress (53 MPa) as compared to that of Specimens GF2, they had a larger maximum axial strain (1.18%) than the former specimens. The axial strain of Specimens GP40 increased by 21.31 % as compared to that of Specimens GF2 as can be seen from Fig. 4b. At the meantime, Specimens GF31 reached both a higher maximum axial stress (60 MPa) and axial strain (1.02 %) as compared to Specimen GF2 (Fig. 4c).

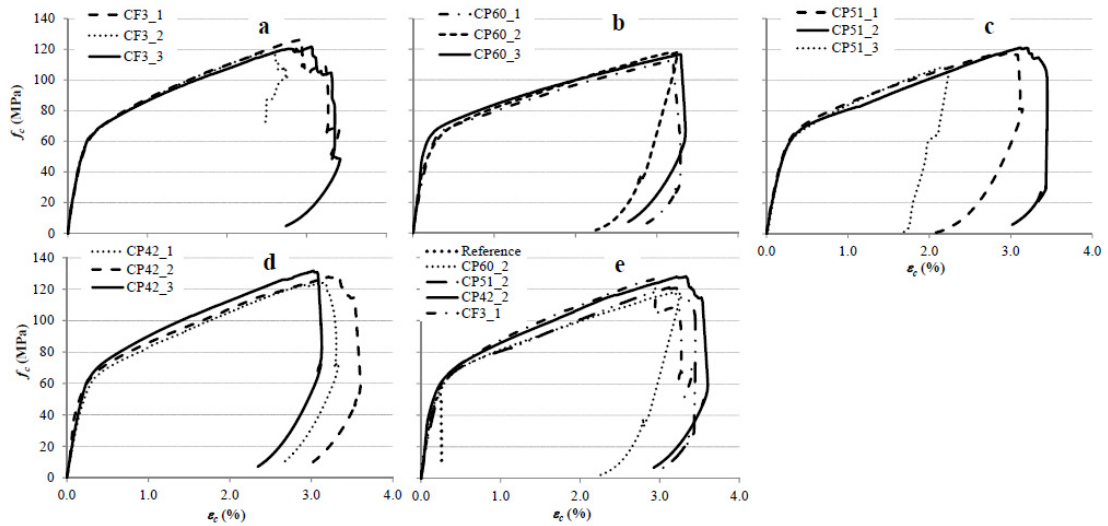


Fig. 5: Stress-strain curves of specimens wrapped by equivalent of three layers

The specimens wrapped with an equivalent of three layers of FRP had similar stress-strain curves but exhibited a slight difference in the axial stiffness for the whole loading process as shown in Fig. 5. Specimens CF3 reached the average maximum axial stress and strain at 122 MPa and 2.84%, respectively (Fig. 5a). The partially wrapped Specimens CP60 again had a lower compressive strength but higher axial strain as compared to those of Specimens CF3. As can be seen in Fig. 5b, Specimens CP60 failed at the average compressive strength of 116 MPa and axial strain of 3.25%. The axial strain for the specimens CP60 increased by 14% in comparison with Specimens CF3. In order to compare the effectiveness of different wrapping arrangements, the stress-strain curves of five specimens were plotted in Fig. 5e. In reference to this Fig., it can be seen that the partially wrapped Specimens CP60 experienced a lower maximum stress and a higher maximum strain, as compared to Specimens CF3.

## 5. Conclusions

In this study the same amount of FRP was used in each group of specimens but with different wrapping arrangements in order to investigate the confinement efficacy between fully, partially and a proposed non-uniform wrapping arrangement for FRP-confined concrete. The findings presented in this study are summarized as follows:

For heavily FRP-confined specimens (CF3, CP60, CP51 and CP42), partial and non-uniform wrapped specimens provides a higher axial strain as compared to that of fully wrapped specimens.

For specimens belonging to the descending branch type, the partially wrapped specimens have a lower compressive strength but a higher strain as compared to the corresponding fully wrapped specimens. On the other hand, the non-uniform wrapped specimens experienced both a higher compressive strength and axial strain in comparison with the fully wrapped specimens.

The partial wrapping arrangement changes the failure modes of the specimens. If the FRP jackets are strong enough, the angle of the failure surface significantly reduces.

The actual rupture strain of the FRP jackets is different for each wrapping arrangement. The strain efficiency factor in the full wrapping arrangement is greater than that of the partial wrapping arrangement but is less than that of the non-uniform wrapping arrangement.

Finally, this study investigated and provided some recommendation on the application of different wrapping arrangements.

## References

- [1] ACI 440.2R-08, Guide for the Design and Construction of Externally Bonded FRP Systems for Strengthening Concrete Structures, American Concrete Institute, Farmington Hills, MI 2008.
- [2] Fib, Externally bonded FRP reinforcement for RC structures, Bulletin, 14,2001, p. 138.
- [3] TR 55, Design guidance for strengthening concrete structures using fibre composite materials, Concrete Society, Camberley,2012.
- [4] Mander, J. B., Park, R., and Priestley, M. J. N., Theoretical Stress-Strain Model for Confined Concrete, Journal of Structural Engineering, 114(8),1988, p. 1804.
- [5] Pham, T. M., Hadi, M. N. S., and Youssef, J., Optimized FRP Wrapping Schemes for Circular Concrete Columns, Journal of Composites for Construction, 2015.
- [6] De Luca, A. and Nanni, A., Single-Parameter Methodology for the Prediction of the Stress-Strain Behavior of FRP-Confined RC Square Columns, Journal of Composites for Construction, 15(3), 2011, p. 392.
- [7] Pham, T. M. and Hadi, M. N. S., Predicting Stress and Strain of FRP Confined Rectangular/Square Columns Using Artificial Neural Networks, Journal of Composites for Construction 2014a, 18(6).
- [8] Pham, T. M. and Hadi, M. N. S., Stress Prediction Model for FRP Confined Rectangular Concrete Columns with Rounded Corners, Journal of Composites for Construction 2014b, 18(1).
- [9] Teng, J. G., Jiang, T., Lam, L., and Luo, Y. Z., Refinement of a Design-Oriented Stress-Strain Model for FRP-Confined Concrete, Journal of Composites for Construction, 13(4), 2009,p. 269.
- [10] Wu, Y. F. and Zhou, Y. W., Unified Strength Model Based on Hoek-Brown Failure Criterion for Circular and Square Concrete Columns Confined by FRP, Journal of Composites for Construction, 14(2), 2010, p. 175
- [11] Lam, L. and Teng, J. G., Design-oriented stress-strain model for FRP-confined concrete, Construction and Building Materials, 17(6-7), 2003,p. 471.
- [12] Pham, T. M. and Hadi, M. N. S., Strain Estimation of CFRP Confined Concrete Columns Using Energy Approach, Journal of Composites for Construction 2013, 17(6).
- [13] Sheikh, S. A. and Uzumeri, S. M., Strength and ductility of tied concrete columns, Journal of the structural division, 106(5),1980 p. 1079.